iScience

CellPress
OPEN ACCESS

Article

Borrelia-specific antibody profiles and complement deposition in joint fluid distinguish antibiotic-refractory from -responsive Lyme arthritis

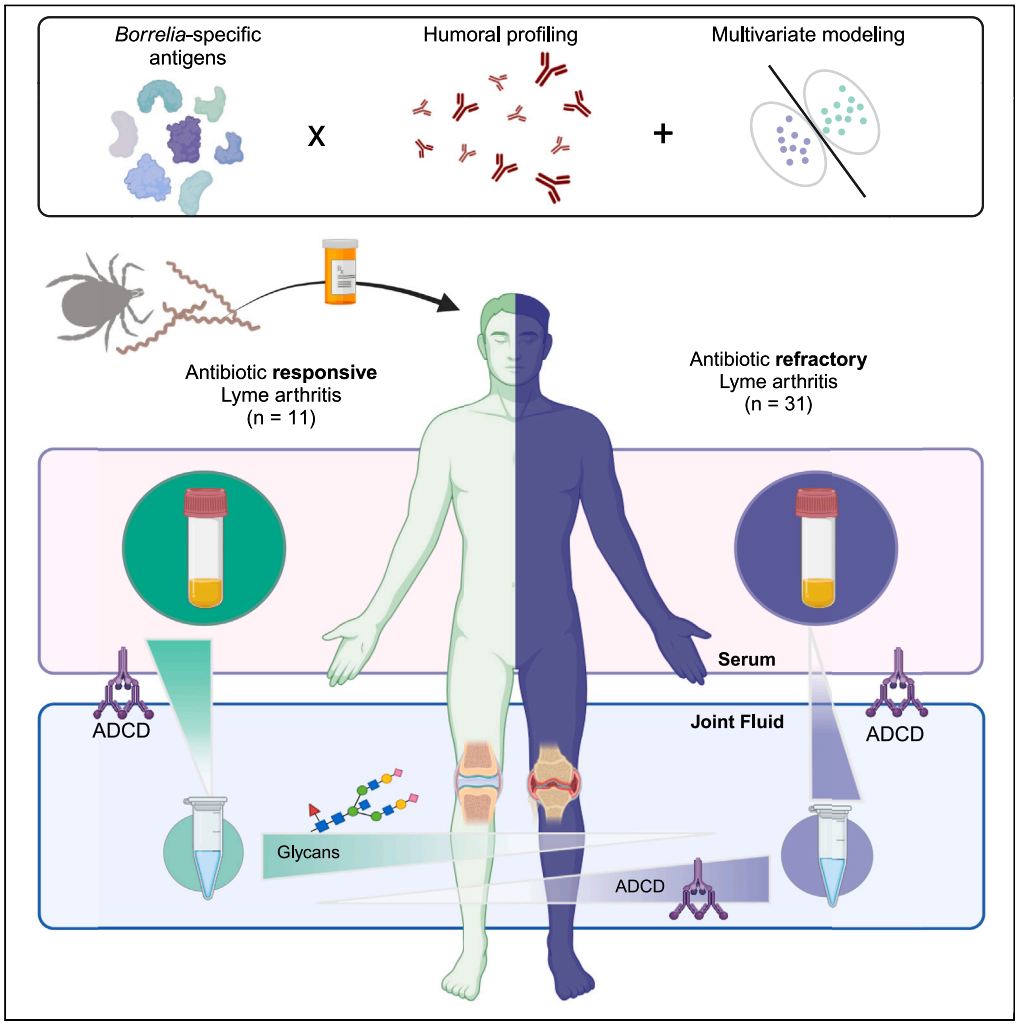

Kathryn A. Bowman, Christine D. Wiggins, Elizabeth DeRiso, ..., Allen C. Steere, Douglas A. Lauffenburger, Galit Alter

asteere@mgh.harvard.edu (A.C.S.)
lauffen@mit.edu (D.A.L.)
galit.alter@modernatx.com (G.A.)

Highlights

Antibody profiles differentiate antibiotic-responsive vs. -refractory Lyme arthritis

Multivariate models discriminate antibiotic-responsive patients in joint fluid only

Serum antibodies alone poorly discriminate antibiotic responsiveness of arthritis

Antibody-dependent complement deposition is dysregulated in refractory patients

Bowman et al., iScience 27, 108804
February 16, 2024
https://doi.org/10.1016/j.isci.2024.108804

iScience

CellPress
OPEN ACCESS

Article

Borrelia-specific antibody profiles and complement deposition in joint fluid distinguish antibiotic-refractory from -responsive Lyme arthritis

Kathryn A. Bowman,[1,2,9] Christine D. Wiggins,[3,9] Elizabeth DeRiso,[1] Steffan Paul,[4] Klemen Strle,[5] John A. Branda,[6] Allen C. Steere,[7,*] Douglas A. Lauffenburger,[3,10,*] and Galit Alter[1,8,*]

SUMMARY

Lyme arthritis, caused by the spirochete *Borrelia burgdorferi*, is the most common feature of late disseminated Lyme disease in the United States. While most Lyme arthritis resolves with antibiotics, termed "antibiotic-responsive", some individuals develop progressive synovitis despite antibiotic therapy, called "antibiotic-refractory" Lyme arthritis (LA). The primary drivers behind antibiotic-refractory arthritis remain incompletely understood. We performed a matched, cross-compartmental comparison of antibody profiles from blood and joint fluid of individuals with antibiotic-responsive (n = 11) or antibiotic-refractory LA (n = 31). While serum antibody profiles poorly discriminated responsive from refractory patients, a discrete profile of *B.burgdorferi*-specific antibodies in joint fluid discriminated antibiotic-responsive from refractory LA. Cross-compartmental comparison of antibody glycosylation, IgA1, and antibody-dependent complement deposition (ADCD) revealed more poorly coordinated humoral responses and increased ADCD in refractory disease. These data reveal *B.burgdorferi*-specific serological markers that may support early stratification and clinical management, and point to antibody-dependent complement activation as a key mechanism underlying persistent disease.

INTRODUCTION

Lyme disease, the most common vector-borne disease in the United States and Europe,[1] is caused by tickborne spirochetes in the *Borrelia burgdorferi* sensu lato complex. With greater than 450,000 cases of Lyme borreliosis estimated annually in the United States,[2] Lyme disease and its post-infectious sequelae contribute to a significant global burden of suffering, economic impact, and disability.

Lyme disease is capable of manifesting in a variety of sites, with multiple possible infectious and post-infectious sequelae. In early localized disease, patients may present with an expanding skin lesion, known as erythema migrans,[3] often accompanied by flu-like systemic symptoms including fever, malaise, fatigue, myalgias, and arthralgias. In the United States, the most common feature of late disseminated disease, Lyme arthritis (LA), is seen in approximately 60% of untreated patients.[3] LA is characterized by mono- or oligoarticular arthritis, often marked by swelling of one or both knees. Because antibiotic treatment of early infection prevents the development of LA, this manifestation of the infection is now seen less commonly.[4] It occurs primarily in individuals whose initial infection was asymptomatic, with arthritis as the presenting symptom.

The natural history of LA is remarkable for its variable response to treatment. Current guidelines from the Infectious Diseases Society of America recommend treatment with a 28-day course of oral antibiotics (doxycycline or amoxicillin).[5] If symptoms persist, repeat treatment with oral antibiotics or a 2–4 weeks course of intravenous (IV) ceftriaxone is recommended. For most patients, symptoms resolve following either oral or IV antibiotic treatment; these are defined as "antibiotic-responsive" LA.[4,6] However, a small percentage of patients have minimal, if any response to oral antibiotic therapy.[6] In most of these minimally responsive or unresponsive patients, joint swelling improves considerably with IV antibiotic therapy, but in some individuals, the arthritis changes after oral and IV antibiotic therapy, and massive synovial hypertrophy develops and persists for months to several years.[7,8] Those cases which fail to improve on oral and IV antibiotic therapy are

[1]Ragon Institute of MGH, MIT, and Harvard, Cambridge, MA 02139, USA
[2]Brigham and Women's Hospital, Division of Infectious Diseases, Boston, MA 02115, USA
[3]Department of Biological Engineering, Massachusetts Institute of Technology, Cambridge, MA 02142, USA
[4]Marks Group, Department of Systems Biology, Harvard Medical School, Boston, MA, USA
[5]Tufts University School of Medicine Boston, Boston, MA, USA
[6]Department of Pathology, Massachusetts General Hospital, Boston, MA, USA
[7]Center for Immunology and Inflammatory Diseases, Massachusetts General Hospital, Harvard Medical School, Boston, MA 02114, USA
[8]Moderna Therapeutics Inc., Cambridge, MA 02139, USA
[9]These authors contributed equally
[10]Lead contact
*Correspondence: asteere@mgh.harvard.edu (A.C.S.), lauffen@mit.edu (D.A.L.), galit.alter@modernatx.com (G.A.)
https://doi.org/10.1016/j.isci.2024.108804

hereafter referred to as "antibiotic-refractory" LA.[9] Physicians treat this complication of the infection with immunosuppressive, disease-modifying anti-rheumatic drugs (DMARDs) and have not seen breakthrough infection in these patients after oral and IV antibiotics, suggesting that this complication of the illness is a post-infectious process. However, in the absence of defined biomarkers able to predict non-responsiveness to antibiotics as well as incompletely defined mechanisms of persistent disease, treatment and management approaches for persistent disease have been variable.

The pathogenesis of antibiotic-refractory LA is not fully understood and is suspected to involve both pathogen- and host-directed processes. While *B. burgdorferi* DNA is typically detectable in synovial fluid by PCR prior to antibiotic therapy, demonstrating the organism's tropism for the joints, PCR results are usually negative after several weeks of antibiotic therapy, and consistently negative in synovial tissue obtained at synovectomy.[10] However, certain spirochetal remnants may persist in the post-infectious period. For example, an important driver of innate immune responses may be the persistence of *B. burgdorferi* peptidoglycan in synovial fluid, which is especially difficult to clear, and may remain detectable long after PCR negativity.[11] Despite the possibility of persistent peptidoglycan, the persistence and progression of synovitis in the absence of live spirochetes in the joint argues against the role of active infection as a primary driver of post-antibiotic synovitis. Instead, it is likely that the pathogenesis of antibiotic-refractory LA is driven by persistent maladaptive immune responses, triggered initially by joint infection.

The basic pathogenetic feature of antibiotic-refractory LA is the development of an excessive and dysregulated pro-inflammatory immune response during the infection, characterized by exceptionally high levels of IFNg and inadequate levels of the anti-inflammatory cytokine IL-10, which persist in the post-infectious period after oral and IV antibiotic therapy.[12] The consequences of this excessive proinflammatory response in Lyme synovia include vascular damage, autoimmune and cytotoxic processes, and fibroblast proliferation and fibrosis.[7] The synovial lesion in these patients is similar with that seen in other forms of chronic inflammatory arthritis, including rheumatoid arthritis, though there is greater vascular damage in post-infectious Lyme synovia.[7,13] For example, in approximately 50% of such patients, Lyme synovia show obliterative microvascular lesions, in which $CD8^+$ T cell-mediated cytotoxicity, $CD4^+$ T cell help, autoantibodies to vascular antigens, and complement deposition may each have a pathogenic role.[14] Additionally, both autoreactive and *B.burgdorferi*-specific humoral immune responses may be modulated by inhibitory FcγR2b, which human and animal models support as a regulator of the quality and magnitude of the humoral immune response.[15]

In LA patients, robust anti-*B. burgdorferi* antibody responses develop to as many as 89 spirochetal proteins, many of which are outer-surface lipoproteins.[16] Additionally, in one study, antibody responses to *B. burgdorferi* sonicate, which is inclusive of both outer-surface lipoproteins as well as intracellular proteins, tended to be higher in patients with refractory LA than in those with antibiotic-responsive LA, but the differences were not statistically significant.[17] Anti-borrelial antibodies are predominantly T cell-dependent IgG1 and IgG3 isotypes, which are capable of inducing opsonization and activating complement.[18] However, the role of *B. burgdorferi* antibodies in protection or pathology remains incompletely defined, and no diagnostic test has been developed which clearly differentiates patients with antibiotic-responsive LA from those at risk for the development of antibiotic-refractory LA.

Emerging data point to qualitative differences in pathogen-specific antibodies, rather than simple antibody levels, as key predictors of protection against bacterial disease progression, such as tuberculosis,[19,20] as well as in protection against complex parasites, including malaria.[21] Thus, here we sought to define whether a comprehensive analysis of *B. burgdorferi*-specific antibody Fc-profiles, along with one Lyme-associated auto-antigen-specific antibody Fc-profile, could classify responders or non-responders to antibiotic treatment. While comprehensive antibody profiling in the serum was unable to discriminate between antibiotic-responsive and antibiotic-refractory individuals, Lyme disease-specific humoral immune responses were significantly divergent between the blood and synovial fluid of both antibiotic responders and non-responders. Moreover, Lyme disease-specific antibody responses differed significantly in the joint fluid across the groups, marked by perturbed antibody Fc-glycosylation across the groups, elevated flagellin-specific responses in antibiotic responders, and greater antibody-dependent antibody-mediated complement activation in the joints of individuals with refractory disease. Consistent with compartmentalization of cytokine and T cell responses noted previously in affected joints,[22,23] these data point to significant joint-specific compartmentalization of humoral immune responses during and following *B. burgdorferi* infection that may point to additional mechanisms driving refractory arthritis at the site of persistent pathogenesis.

RESULTS

Minimal univariate differences between antibiotic-responsive and antibiotic-refractory individuals

Biophysical profiling of *Borrelia burgdorferi* (*Bb*)-specific antibodies to B67 culture lysate (derived from strain B39/40), CRASP1, CRASP2, DbpA, DbpB, Arp37, flagellin, OspA, OspB, OspC, OspE, p27, p35, p39, VlsE (all recombinant Bb proteins are based on strain B31, an OspC type A (RST1) strain), and autoantigen-specific apolipoprotein B100 (ApoB100) was performed in matched serum and joint fluid from 31 individuals with antibiotic-refractory LA and 11 individuals with antibiotic-responsive LA (Table 1). In patients with antibiotic-responsive LA, paired joint fluid and serum samples were obtained before or during oral antibiotic therapy, whereas samples in the patients with antibiotic-refractory LA were collected near the time of IV antibiotic therapy.

Univariate comparison of antibody isotype-specific responses across traditional *Bb* antigens, OspA and flagellin, in serum, showed no significant differences between antibiotic-refractory and antibiotic-responsive individuals (Figure 1). Similarly, antibody isotype levels to the same antigens showed limited differences in joint fluid across the groups (Figure 1). At a univariate level (Figure S1), a significantly higher level of FcγR2A-binding *Bb* p35-specific antibodies was observed among responders compared to non-responders (Figure 1). Moreover, holistic antibody profiling revealed additional differences in the overall humoral immune response across the groups (Figure 1). Notably, while each

Table 1. Clinical characteristics of antibiotic responsive and antibiotic refractory Lyme arthritis patients

	Antibiotic responsive LA N = 11	Antibiotic refractory LA N = 31
Age, median (range), years	47 (19–70)	39.5 (12–78)
Sex, no. female: no. male	2 : 9	14 : 17
***B. burgdorferi* infection**		
Bb IgG titer median (range)	25,600(1,600-102,400)	25,600 (400-102,400)
Bb JF PCR (positive/total tested)	2/10	1/24
Inflammatory markers, median (range)		
ESR	26 (8–60)	10 (2–87)
CRP	15.2 (8.1–121.6)	5.6 (0.4–105.7)
HLA-DRB1 risk alleles[a]		
Patients with at least one high risk DRB1 type/total tested (%)	4/10 (40%)	18/28 (64%)
Antibiotic treatment duration, median (range)		
All antibiotics prior to sample, days	36 (0–160)	123 (1–602)***
# resolved with oral antibiotics (%)	4/11 (36%)	N/A
# resolved with IV antibiotics (%)	7/11 (64%)	N/A
IV antibiotics prior to sample, days	0	40 (0–612)***
Arthritis characteristics		
Total duration arthritis, median (range), months	6.5 (3.3–12.2)	13.7 (5.1–76+)***
JF characteristics, median (range)		
WBC count	10,481 (285-27,922)	12,150 (3,475-30,750)
% neutrophils	82 (7–92)	76.5 (0–98)
% lymphocytes	9.5 (0–28)	14 (0–81)

LA = Lyme arthritis, *Bb* = *B. burgdorferi*, JF = joint fluid, ESR = erythrocyte sedimentation rate, n/a = not applicable, CRP = C-reactive protein, WBC = white blood cell.

*p < 0.1, **p < 0.05, ***p < 0.01.

[a]High risk for antibiotic refractory LA: DRB1*0101, 0401, 0402, 0404, 0405.

individual possessed a unique Lyme-specific Fc-profile, decreased sialylation (detected by binding of sambucus nigra lectin—SNA) and galactosylation (detected by binding of Ricinus communis agglutinin 1—RCA) was observed in the joint fluid of individuals with refractory infection, although these univariate differences did not rise to the level of statistical significance. Additionally, antibodies to only 8 antigens were targeted by secretory-IgA (secIgA) detected solely in the joint fluid—including responses to DbpA, DbpB, flagellin, OspA, OspB, B67 lysate, VlsE, and p39. Thus, consistent with previous reports, limited univariate differences were observed in the overall magnitude of *Bb*-specific antibody titers, across responders and non-responders to antibiotics in the serum, but subtle differences were noted in the joint fluid *Bb*-specific antibody profiles across the groups.[17,24]

Cross-compartmental antibody signatures vary by antibiotic responsiveness

Given the observation of subtle antibody differences across the groups at a univariate level, particularly among Fc-modified *Bb*-specific antibodies in the synovial fluid, we next sought to define whether overall compartment-specific differences existed across the groups. Thus, focusing on the features that showed some difference in the heatmap, polar plots were generated across each antigen, representing the mean percentile rank for each antigen-specific feature (Figures 2A—2D, S3, and S4). Strong compartment-specific effects were observed, as expected, marked by reduced sialylation (SNA) and galactosylation (RCA) in the joint across antigens (Figures 2A—2D), as well as reduced IgG1, IgG2, IgM (Figure S3), and FcγR binding (Figure S4) in the serum, pointing to the selective recruitment of more inflammatory antibody profiles, notable for decreased sialylation and galactosylation, in the joint across both groups.[25,26] Conversely, higher levels of IgA and secretory IgA (secIgA) were observed in the joint fluid in both groups compared to the serum (Figure S3). However, complement-activating antibodies, able to elicit antibody-dependent complement deposition (ADCD), were markedly discordant across the compartments and across groups, with enhanced complement-activating antibodies in the joint fluid in individuals with refractory LA and diminished levels in the joint fluid in individuals with responsive LA (Figures 2A—2D). Thus, these data indicate clear compartment-specific differences in *Bb*-specific antibody profiles, marked by more inflammatory antibodies (less sialic acid and galactose) in the joints of refractory infections, diminished IgA

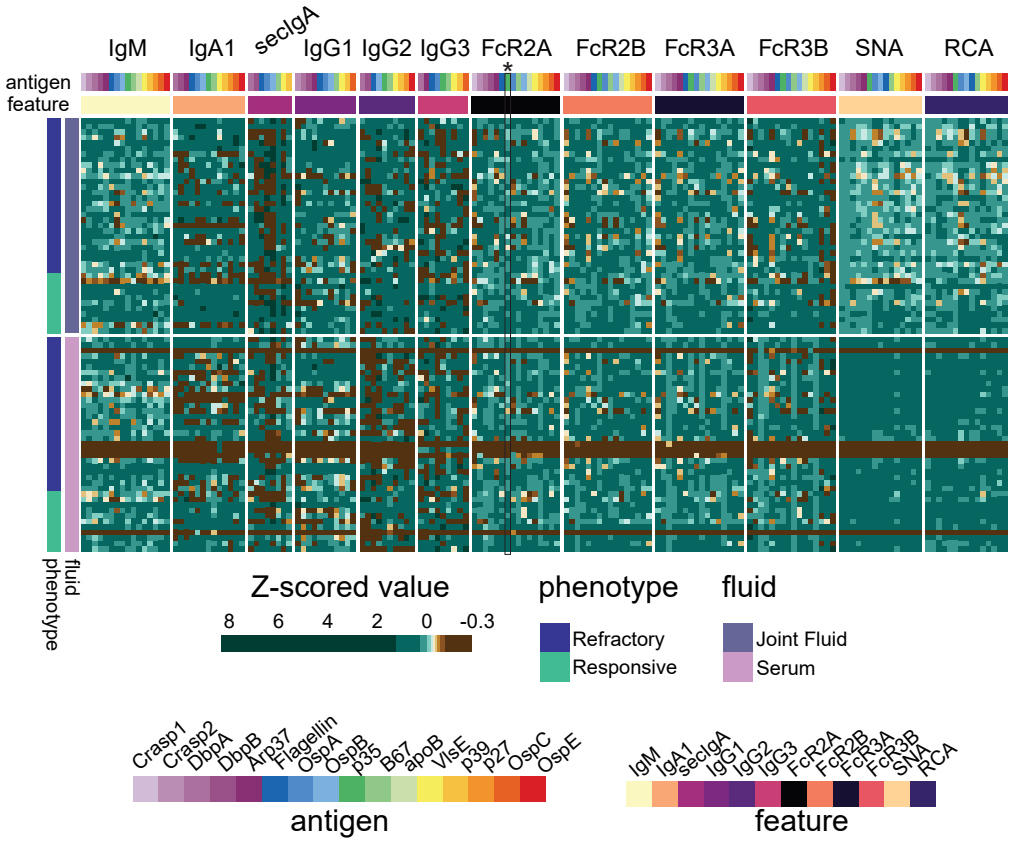

Figure 1. Systems serology profiling with *Borrelia*-specific antigens reveals patient heterogeneity

The heatmap shows the *Z*-scored measurements for 12 features, across 16 antigens for both refractory and responsive patients, visualized with joint fluid measurements in the upper half of the heatmap and serum measurements in the lower half of the heatmap. Only antigens detected above background for at least 30% of samples were included for each measurement. Statistical significance was assessed using the Mann-Whitney nonparametric test, with p values then corrected for multiple hypothesis testing via Benjamini-Hochburg, *p < 0.05, **p < 0.01, ***p < 0.001, else not significant.

responses, and expanded complement activation in the joints of individuals with refractory infections, collectively pointing to the persistence of a highly compartment-specific inflammatory response that may mark or drive pathology.

Multivariate antibody profiles in joint fluid, but not serum, can discriminate antibiotic-resistant from antibiotic-responsive LA

Given the trend toward FcR differences across the groups in univariate analyses and distinct patterns emerging in the correlation networks, we next aimed to determine whether a multivariate antibody Fc-profile, reflective of differences in the polyclonal pools of antibodies present in a given individual, could distinguish the groups. Given the highly correlated nature of the humoral immune response following infection, where B cells expand in response to multiple antigens simultaneously, we first used a least absolute shrinkage and selection operator (LASSO) regularization to conservatively down select the number of features utilized for model building to avoid statistical overfitting.[27,28] These LASSO-selected features were then used to build a partial-least squares discriminant analysis (PLS-DA) model to separate groups. When a PLS-DA model was built with LASSO-selected serum antibody features (Figure 3A), the model could not resolve the 2 groups, suggesting that serum antibody responses were similar between phenotypes. However, when a model was built with joint fluid features only (Figure 3B), responsive and refractory groups separated well. The joint fluid-specific model was able to differentiate antibiotic refractory from responsive individuals (Figure S5B), with a cross-validation accuracy of 0.84, determined with 100 rounds of 5-fold cross-validation (Figure S5A).

To gain deeper insights into the specific features that separated the groups, PLS-DA weights for the LASSO-selected features were plotted (Figure 3C), highlighting that as few as 9 of the overall 167 features that were analyzed per sample were required to discriminate between joint fluid profiles in responsive and refractory individuals. The 9 features included 6 features that were selectively enriched in the responsive group and 3 features that were selectively expanded in the refractory subjects. The responsive features included elevated p35-specific antibodies able to bind to the activating opsonophagocytic FcγR2A receptor, elevated levels of galactosylated (detected by RCA binding) flagellin- and *Bb*-derived Arp37-specific antibodies, sialylated (detected by SNA binding) flagellin-specific antibodies, IgG2 responses to flagellin, and IgG3 responses to p39, pointing to a highly flagellin, p35, p39, and Arp37-specific response in individuals that respond to antibiotics.

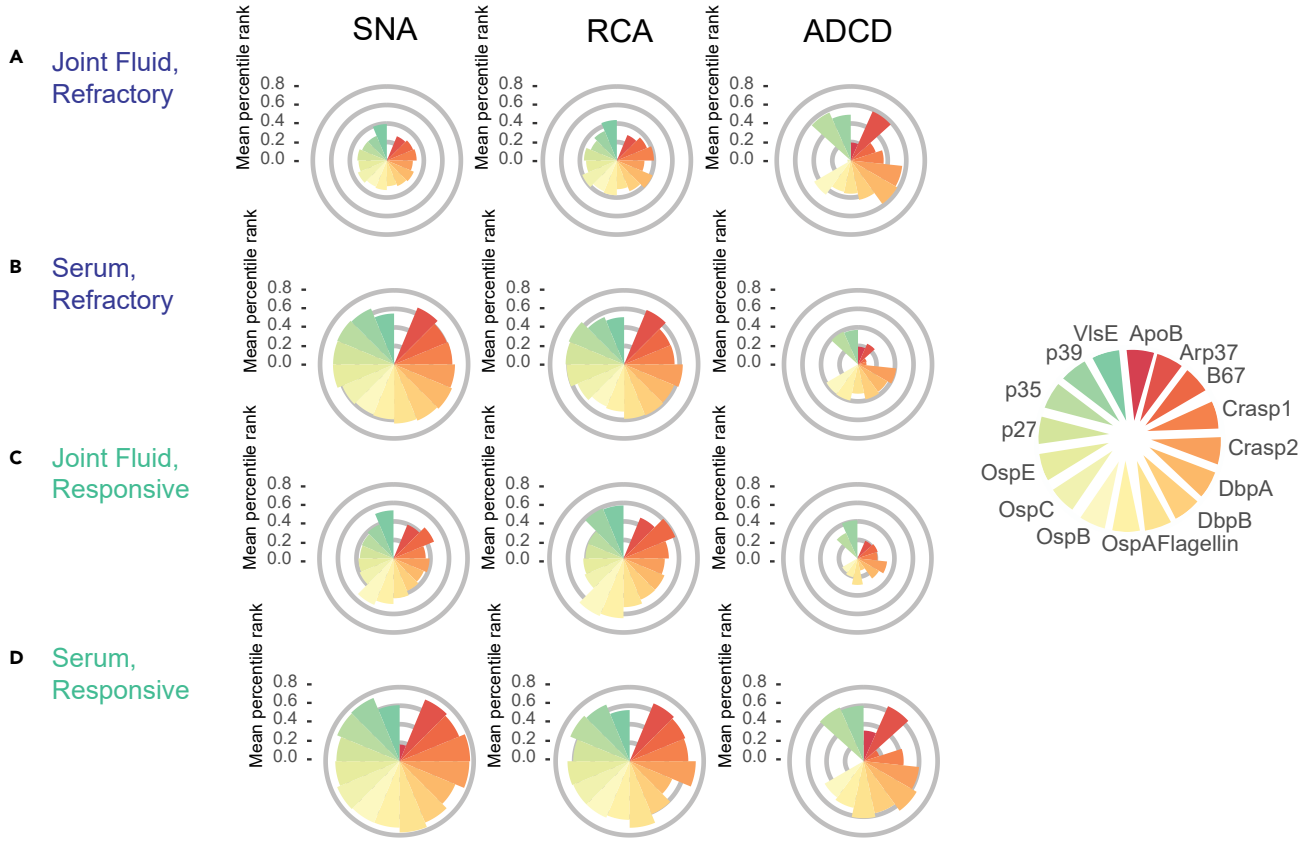

Figure 2. Compartment-specific responses differ across antibiotic responsiveness

The polar plots show the mean percentile rank for each antigen for sambucus nigra (SNA) lectin binding, Ricinus communis agglutinin 1 (RCA) lectin binding, and antibody-dependent complement deposition (ADCD) measurements for (A) refractory joint fluid, (B) refractory serum, (C) responsive joint fluid, and (D) responsive serum. The antigen key indicates the corresponding antigen for each colored slice of the polar plot.

Conversely, 3 features were enriched in individuals that were refractory to antibiotics, including elevated *Bb*-derived p39 and DbpA-specific antibodies able to bind to the inhibitory FcγR2b receptor, and elevated levels of lysate (B67)-specific complement-fixing antibodies, highlighting a highly divergent complement fixing and inhibitory Fc-receptor binding response in the joint fluid of individuals that have persistent arthritis despite antibiotic therapy.

Because LASSO feature selection picks a minimum set of features, that maximally represents the variation across the groups, we next generated a LASSO feature-co-correlate network from the joint fluid (Figure 3D) to define additional antibody measurements that are highly correlated with the LASSO-selected features and which may provide additional biological insights into disease pathobiology. Specifically, alterations in DbpB-specific antibody glycosylation were linked to altered flagellin-specific antibody glycosylation profiles, with a specific elevation in galactosylation (higher RCA binding) and sialylation (higher SNA binding) in responsive LA. Interestingly, multiple additional DbpA and DbpB FcγR binding levels were associated with LASSO-selected DbpA and DbpB FcγR measurements, pointing to a unique role of highly functional Dbp responses in Lyme pathology.

Cross-compartmental comparisons reveal differential antibody profiles in the joint in refractory and responsive disease

Given the distinct antibody responses seen across compartments, we sought to finally define whether any particular type of antibody measurement could best resolve clinical outcome groups. A pan-antigen score, combining all *Bb* antigen-specific measurements for a given antibody readout (Figure 4A), was created and compared across compartments within each group. In refractory disease, all antibody subclasses showed significantly higher pan-antigen scores in the joint fluid than in the serum, but no such differences were observed in responsive patients (Figures 4B and S6). In contrast, ADCD levels in responsive patients were broadly higher in serum as compared to joint fluid, whereas in refractory patients, ADCD levels were higher in joint fluid than in serum, likely related to the higher ADCD levels observed for VlsE, p39, DbpA, DbpB, and B67 lysate in refractory joint fluid (Figure 2A).

To further explore the specific features that were most distinct across the compartments in each group of subjects, a multilevel PLS-DA model built on LASSO-selected features was used in individuals with refractory disease (Figure 5A) or responsive infection (Figure 5B). Complete separation was observed across the compartments in both groups, but compartments were marked by different antibody

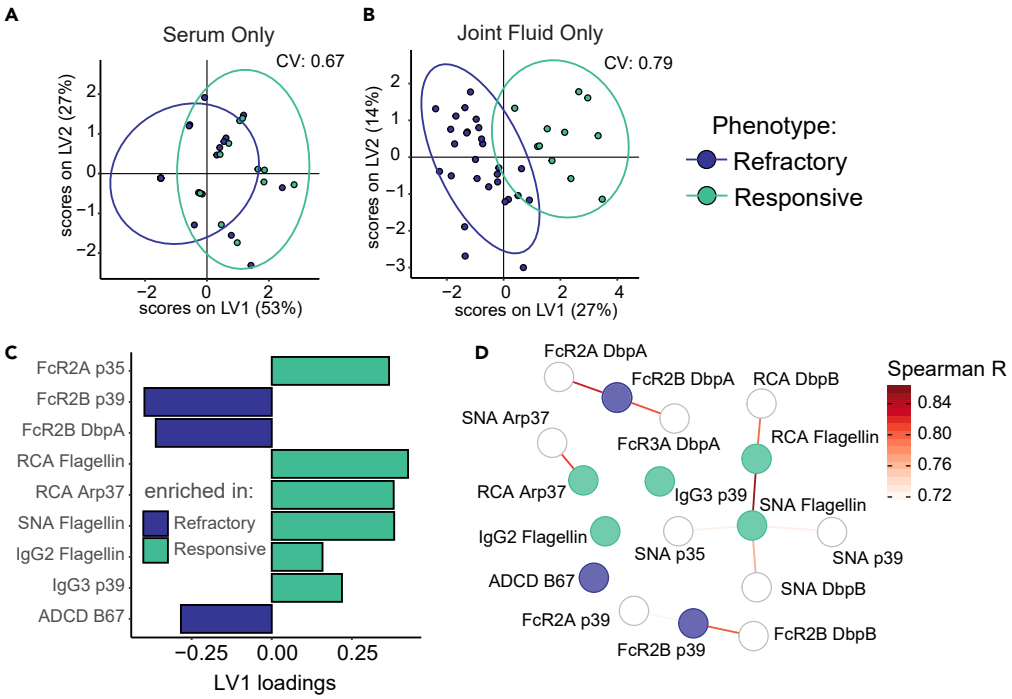

Figure 3. Multivariate modeling discriminates antibiotic responsive patients in joint fluid but not serum

Partial-least squares discriminant analysis (PLS-DA) models were built using selected features on (A) serum data alone or (B) joint fluid data alone. The dot plots show the resultant scores of each sample on latent variables 1 and 2, with ellipses representing the 95% confidence intervals of the refractory (dark blue) and responsive (green) groups. LV labels represent X block variation captured. (A) utilized elastic net feature selection with alpha = 0.4 and lambda = 0.278 after tuning, while (B) utilized LASSO feature selection. The choice of feature selection algorithms differed in order to force the selection of multiple features in the serum-only model for appropriate comparison.

(C) The bar graph shows the loadings of LASSO-selected features for (B) on latent variable 1 (LV1), with bar colors indicating in which group the feature is enriched (dark blue for refractory, green for responsive).

(D) A pairwise Spearman correlation test was performed to determine features that were correlated with the LASSO-selected features visualized in (C). Features with correlation of coefficients >|0.85| and $p < 0.01$ are shown in the networks. Spearman correlation strength is represented by line color, indicated by inset Spearman R legends. Node color indicates in which group the feature is enriched (dark blue for refractory, green for responsive).

subpopulations. Most LASSO features were enriched in the joints of refractory subjects, including high levels of IgG2s, secretory IgA, FcγR3b binding antibodies and ADCD-inducing antibodies, whereas only OspE-specific FcγR3b binding antibodies were enriched in the serum in these subjects (Figure 5C). Further analysis of the co-correlates of the LASSO-selected features pointed to the accumulation of additional antigen-specific IgG2, IgAs and complement-fixing antibodies in the joints of refractory individuals (Figure 5E). Comparably robust separation was noted between serum and joint fluid in the responsive samples. In both refractory and responsive individuals, separation between fluids was marked by higher levels of flagellin-specific IgG2 and *Bb*-lysate-specific secretory IgA in the joints (Figures 5C and 5D). However, joint fluid in responsive subjects was additionally marked by higher levels of OspA-specific IgA and p39-specific IgG3 (Figure 5D). Conversely, ADCD-inducing antibodies were largely observed in the serum in responsive individuals. Further co-correlates analysis pointed to a highly correlated complement (ADCD) network across antigens in the serum, but a large and highly correlated network of FcγR3b, IgG3, and IgA, all of which trigger neutrophil activity, as a key signature of joint fluid in the setting of responsive infection (Figure 5F). Cumulatively, these data point to significant antibody differences across the compartments, marked by the accumulation of IgA and IgG2 in joints in both groups, but the selective accumulation of complement-fixing antibodies in refractory joints only.

Ranking of antibody features by relative frequency highlights cross-compartmental variation

To ultimately define the particular features that resolved the groups, we evaluated the proportion of individuals in either the responsive or refractory group that generated antibody responses that diverged across the compartments (Figure 6A). Variation was observed in the level of antigen-specific immunity across the antigens, with highly robust targeting of the Dbps but less targeting of p27 and p35 across the antibody readouts (Figure 6A). Only antigen-specific differences in IgG2 responses in refractory patients rose to the level of statistical significance, while no differences were detected in responsive patients, potentially due to low sample numbers. However, ADCD, IgA, and IgG2 responses across the responsive and refractory groups in the serum and joint fluid appeared to reveal consistent trends toward compartment-specific differences, while fewer differences were noted in IgG1 and IgG3 responses. Interestingly, antigens that deviated in the compartments

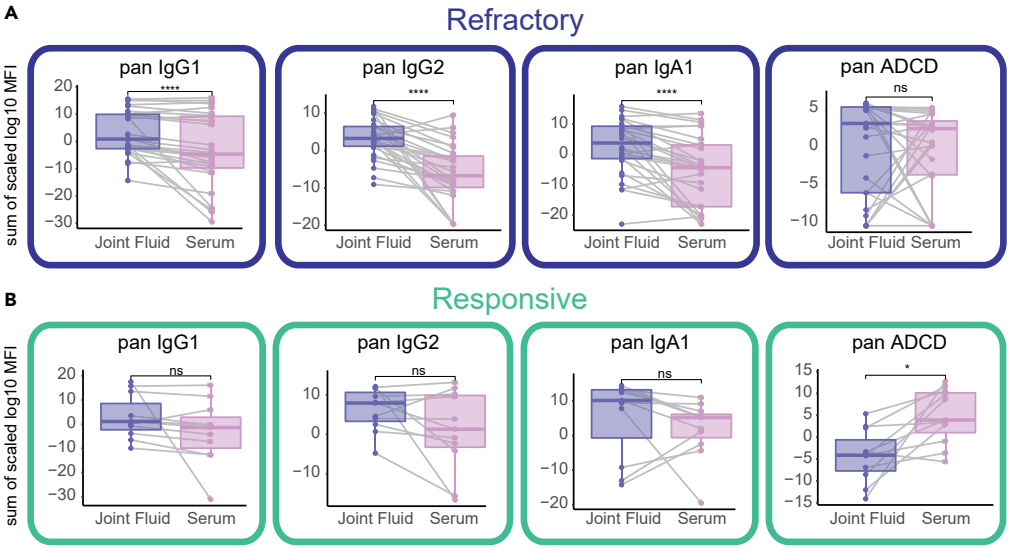

Figure 4. Pan-antigen scores demonstrate that ADCD levels across antigens are discordant between fluids and phenotypes

Select pan-antigen scores are visualized as boxplots for (A) refractory and (B) responsive phenotypes. Paired serum and joint fluid samples are available for each individual, and so significance was tested with a nonparametric Wilcoxon signed-rank test and corrected for multiple hypothesis testing via Benjamini-Hochburg, *p < 0.05, **p < 0.01, ***p < 0.001, ns, not significant. Gray lines connect paired samples.

differed across the groups, with the immunodominant antigens (Dbps and p39) in the serum, but the Osp, B67 lysate, and flagellin antigens in the joints, marking a disconnect in the potential antibody subpopulations and functions that may be associated with prolonged pathology.

However, to identify the antibody profiles that were differentially enriched across compartments in the 2 groups of subjects, a compartment ratio was developed such that numbers <1 indicated a higher proportion of detectable response in joint fluid, and >1 indicating the feature was disproportionately enriched in serum (Figure 6B). In general, refractory patients had lower ADCD, IgG2, and IgA ratios across several *Bb*-antigens indicating a higher proportion of response in the joint fluid. Both ADCD and IgA ratios were collectively statistically significantly lower in refractory patients. Conversely, as expected, no differences in IgG1 detection were noted across the groups. Interestingly although IgG3 varied for only a limited number of antigens and was not significant overall, the ratio of these was inverted from other subclasses, with a relative enrichment of Crasp1, Crasp2, and OspE-targeted IgG3 in the joint fluid of responsive individuals. These data not only collectively point to a selective deficit in complement fixing and IgA immunity in the serum of individuals with refractory LA, providing insights into the specific antibody profiles that may discriminate antibiotic responsiveness after *Bb* infection but also points to unappreciated mechanisms that may underlie protection against Lyme disease.

DISCUSSION

LA is among the most common manifestations of Lyme disease in the US and is notable for its strikingly variable responsiveness to antibiotic therapy, but the mechanisms driving antibiotic-refractory disease remain incompletely defined. Moreover, biomarkers for early identification of patients who will develop persistent synovitis and potential joint damage are lacking. Thus, biomarkers to help guide both clinical management and therapeutic strategies are urgently needed.

Borrelia has evolved a wide range of mechanisms for invasion, dissemination, tissue colonization, and host immune evasion, involving dramatic changes in gene expression.[29,30] The resulting host immune response can cause persistent pathology in a subset of individuals that develop LA.[12] Importantly, immunogenic protein recognition profiling clearly illustrates that the *Bb*-specific humoral immune response is distinct in active Lyme disease as compared to convalescent patients.[16] Similarly, Th1 responses and IgG titers to an immunogenic *Bb* lipoprotein, OspA, have been associated with greater swelling and longer duration of arthritis after antibiotic treatment, pointing to associations between antigen-specific response and severity of disease.[31,32] However, whether precise antibody profiles can predict the evolution of persistent antibiotic-resistant LA remained unclear. Thus, here, by expanding antibody profiling across a wider range of borrelial antigens, as well as profiling the humoral immune response, we observed striking differences in the polyclonal antibody profiles between the serum and joint fluid that diverged in individuals who developed refractory LA compared to those that responded to antibiotics. Strikingly, differences in IgG Fc-glycosylation, which serve as markers of inflammatory potential and can lead to complement activation, were key predictors of differences in clinical progression.[33]

Individuals who developed antibiotic-refractory LA exhibited a distinct joint fluid antibody profile, characterized by the presence of inflammatory antibodies with decreased *Bb*-specific antibody sialylation and galactosylation, decreased IgA responses, and increased complement activation in the joint fluid. Thus, despite the multiple elaborate mechanisms by which *Bb* subverts the complement cascade,[30,34–37] the pathogenesis appears to be related to persistent activation of the complement cascade and thus may be related to a pathogen-induced over-activation of complement in the joint. To contextualize these findings within the broader immune response, a recent study demonstrated

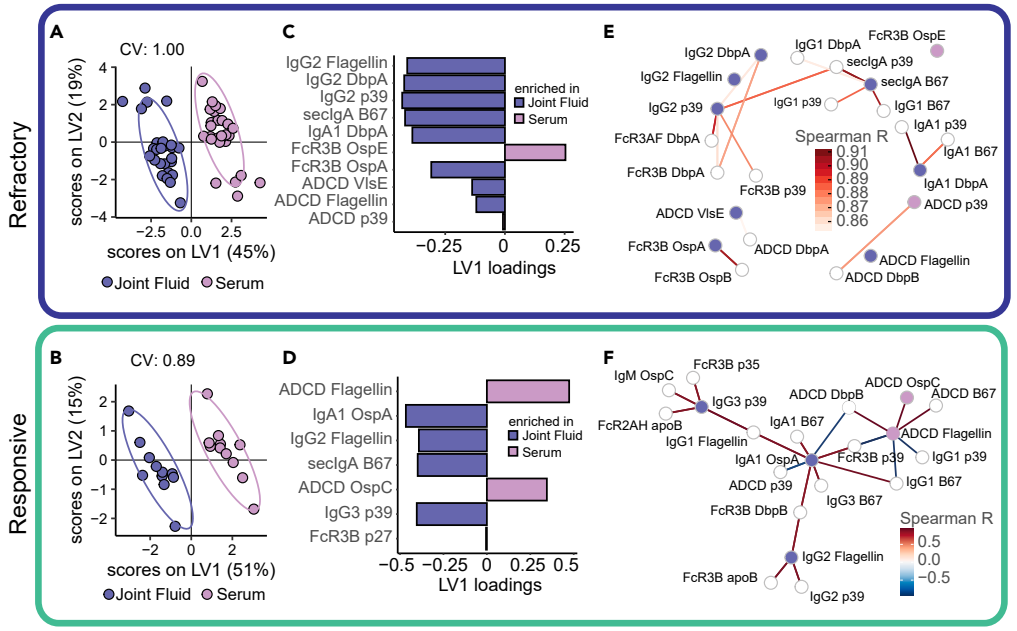

Figure 5. Fluid-specific humoral profiles reveal complement-fixing antibodies partition into antibiotic refractory patient joints but responsive patient serum

(A) Multi-level PLS-DA model using LASSO-selected features was built on (A) refractory joint fluid (purple) and serum (pink) data, and (B) responsive joint fluid (purple) and serum (pink) data to account for the paired data structure. The dot plots show the resultant scores of each sample on latent variables 1 and 2, with ellipses representing the 95% confidence intervals. The 5-fold cross-validation accuracy score is also displayed. The bar graph shows for (C) the refractory group and (D) the responsive group the loadings of LASSO-selected features on latent variable 1 (LV1), with bar colors indicating in which group the feature is enriched (purple for joint fluid, pink for serum). Network plots for the (E) refractory group and (F) responsive group show features highly correlated with the LASSO-selected features, determined through pairwise Spearman correlation tests. Features with correlation of coefficients >|0.85| and $p < 0.01$ are shown in the networks. Spearman correlation strength is represented by line color, indicated by inset Spearman R legends. Node color indicates in which group the feature is enriched (purple for joint fluid, pink for serum). FcR3B p27 correlations are excluded due to its negligible contribution to LV1.

C5b-9 deposition on obliterated blood vessels in the synovia in refractory LA, which correlated with autoantibody responses to certain vascular-associated autoantigens.[14] $CD8^+$ T cells with cytotoxic potential surrounded these vessels and $CD4^+$ T cells were intermixed with $CD8^+$ T cells. Thus, complement activation by pathogen-associated immune complexes, while certainly not the sole contributor to persistent LA, may be implicated in pathology.

How and where antigens persist, enabling the chronic formation of immune complexes, remains unclear. However, the presence of inflammatory complement-fixing antibodies, particularly at the site of pathology, could lead to protracted inflammation and disease. Inadequately controlled complement activation could also drive immunopathogenesis, as seen in multiple inflammatory and autoimmune diseases, including rheumatoid arthritis.[38,39] Specifically, studies of the synovial tissue in rheumatoid arthritis have highlighted the presence of synoviocytes in hyperplastic areas that express C3 receptors and Fcγ receptors, allowing these cells to respond rapidly to immune complexes and trigger inflammation due to their hyper-inflammatory state.[40] Moreover, the observed enrichment of complement-activating antibodies in the joint in refractory LA is consistent with previous studies of borrelial challenge in C3-deficient (C3−/−) mice revealing worsened early control of *Borrelia* infection in C3 knockout mice, but significantly less joint damage weeks after infection in the knockout mice compared to the wildtype animals.[41] These data point to a complex role for complement, critical for early control of the pathogen, but with the need to attenuate the inflammatory activity of the complement system to avoid prolonged pathogenesis. Thus, in the presence of the bacteria, complement evasion machinery may systematically block the inflammatory activity of the complement cascade. However, once the bacteria are cleared, prolonged exposure to immune complexes may contribute to persistent activation and disease. While it is uncertain whether events at the time of pathogen clearance lead to the persistence of complexes in joints that triggers pathology, several complement inhibitors exist that could be tested for a therapeutic impact on alleviating protracted symptomatology.

Changes in pathogen-specific antibody Fc-glycosylation have been noted as significant predictors of disease progression across several infectious diseases including human immunodeficiency virus infection,[42,43] tuberculosis,[19] and SARS-CoV-2 infection,[44–47] as well as several non-infectious diseases.[48] Loss of sialylation and galactosylation is a critical marker of inflammation and likely associated with the presence of highly activated plasmablasts, secreting copious number of inflammatory antibodies aimed at driving rapid pathogen clearance and immune activation to overcome the infection. In a recent report, patients with antibiotic-refractory LA had *Bb* IgG1 antibodies in synovial fluid with proinflammatory glycan profiles, containing high percentages of bisecting GlcNAcs, with intermediate percentages of galactose and fucose, and low percentages of sialic acid.[25] In contrast, patients with antibiotic-responsive LA had *Bb*-specific IgG1 antibody glycans with less

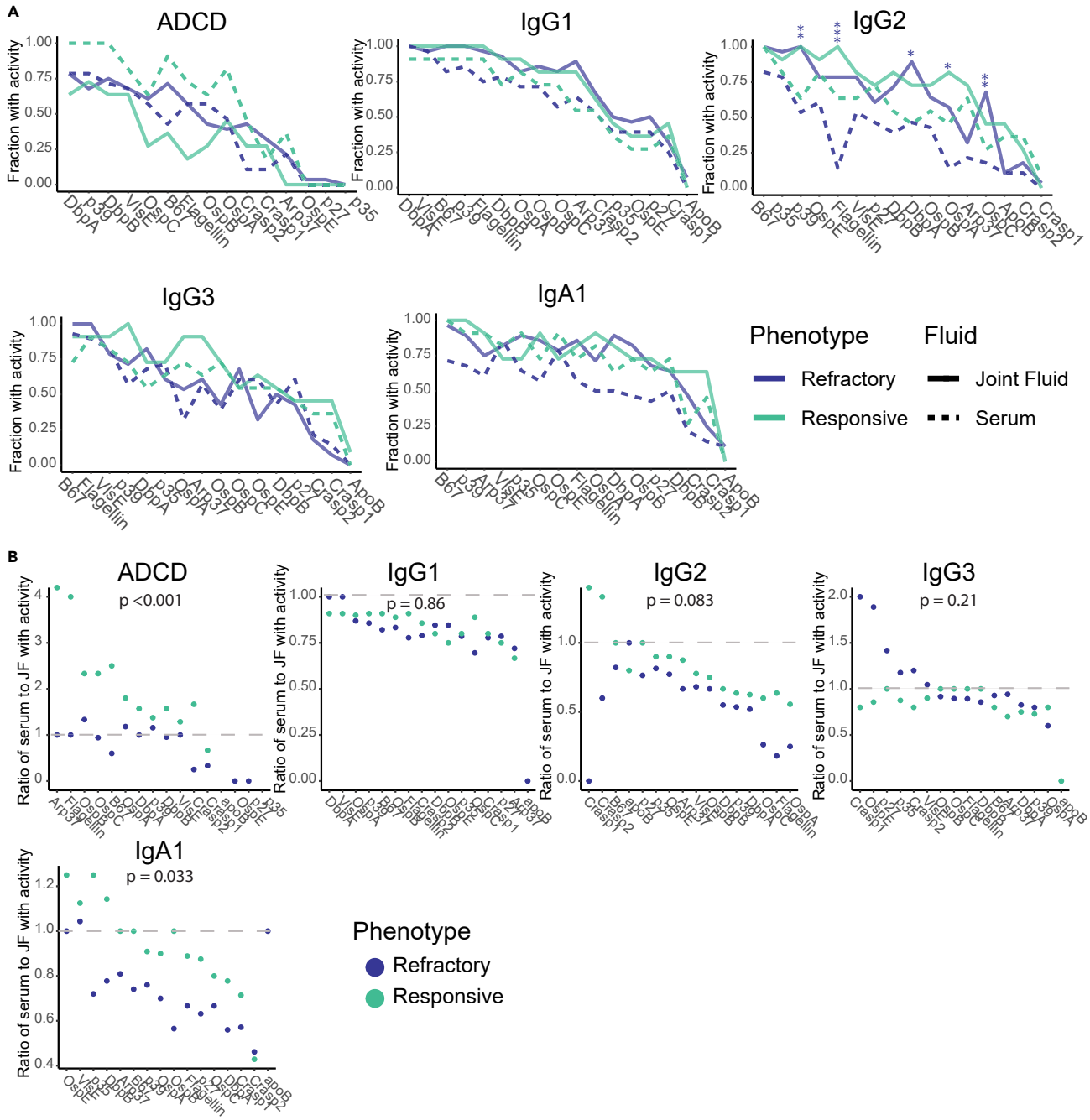

Figure 6. Antigen-specific IgG2, IgA1, and ADCD partitioning between compartments differs significantly across disease phenotypes

(A) Fraction of samples with non-zero measurements for ADCD, IgG1, IgG2, IgG3, and IgA1 for refractory (dark blue) and responsive (green) patients in the serum (dashed line) and joint fluid (solid line) for each antigen. Significant differences in distribution of non-zero measurements between fluids as assessed by a Fisher's exact test are denoted as *$p < 0.05$, **$p < 0.01$, ***$p < 0.001$ for refractory (dark blue) and responsive (green) samples after correction for multiple hypothesis testing via Benjamini-Hochburg.

(B) Ratio of fraction of serum samples with non-zero measurements to fraction of joint fluid samples with non-zero measurements for ADCD, IgG1, IgG2, IgG3, and IgA1 for refractory (dark blue) and responsive (green) patients for each antigen. Significant differences in distributions of ratios between phenotypes are assessed by a Mann-Whitney nonparametric test, then corrected for multiple hypothesis testing via Benjamini-Hochburg.

marked pro-inflammatory profiles reflective of a controlled pro-inflammatory response. Thus, the data presented here suggest that a simple lectin-based analysis of the pro-inflammatory status of *Bb*-specific antibodies in the joint could provide a rapid indication of antibiotic responsiveness. However, at a mechanistic level, whether these glycosylation differences evolve as a result of protracted inflammation or are

themselves the driver of the refractory course is unclear. Similar patterns of glycosylation are observed in multiple autoimmune and infectious diseases,[48] including reduced IgG galactosylation and sialylation patterns in systemic lupus erythematosus,[49,50] and aberrant galactosylation predictive of onset and severity of rheumatoid arthritis.[51–53] Moreover, pro-inflammatory glycosylation can be targeted therapeutically either by infusion of antibodies with glycosylation lacking in the inflamed model,[54,55] or through use of engineered antibodies or intravenous-immunoglobulin with specific glycosylation patterns[26,56] to differentially affect the IgG effector roles of immunoglobulins. It is unclear whether pathogen or simply the persistence of antigen in the joint is sufficient to drive the persistent production of inflammatory antibodies. However, the selective presence of these antibodies points to a pathogen-specific glycan profile that could be used to predict non-responsiveness.

Cross-compartmental profile differences revealed weaker discrimination between groups using serum features, but stronger discrimination of antibiotic-refractory and responsive individuals in joint fluid, pointing to a compartmentalization of pathological antibodies. Coupling LASSO-selected features along with highly correlated features for these groups, the responsive group targeted p35, flagellin, Arp37, p39, VlsE, and apoB100, collectively potentially representing the key targets required for the successful clearance of the pathogen and associated antigens. Conversely, refractory infection was predicted by the evolution of p39 and DbpA-specific antibodies that bind preferentially to the inhibitory FcγR2b receptor that may lead to less profound clearance of the bacteria. Perhaps not surprisingly, responsive joint fluid was notable for a more significant IgM response to multiple borrelial antigens. Interestingly, prior studies have observed a link between prolonged arthritis and the presence of antibodies to two *Bb* antigens, OspA and Osp B,[57] presumably because of the inflammatory potential of *Bb* lipoproteins. Additional evidence of immune compartmentalization has been noted, including significantly higher levels of several cytokines in joint fluid, particularly CXCL9 and CXCL10, in refractory compared with responsive patients. Joint fluid from refractory individuals also had fewer $CD4^+$ $CD25^+$ FoxP3-positive (T regulatory) cells, with increased TNFα and interferon-γ production in refractory compared with responsive patients.[23,58] The data presented here support this model, where the production of inflammatory, persistent complement-activating antibodies, despite negative *Bb* PCRs in most joint fluid tested (96% refractory, 80% responsive), contributes to dysregulated inflammation and prolonged symptomatology, in a compartment-dependent manner.

In addition to enrichment for complement deposition in the joint fluid of refractory individuals, this group was also distinguished by a selective deficit in IgA immunity in the serum and a relative cross-compartmental enrichment for IgA in the joint fluid. IgA immune complexes can bind with high affinity to FcαRI on neutrophils, resulting in excessive neutrophil activation, NETosis, degranulation, and cytokine secretion.[59] If persistent, IgA immune complex-mediated neutrophil activation can drive tissue damage, which has been implicated in pathology in several inflammatory or autoimmune diseases.[60,61] As the predominant cell in joint fluid, neutrophils are critical for spirochetal killing. Thus, similar to complement, IgA-mediated neutrophil activation may represent an initially protective mechanism important for eradication of the pathogen, which may become dysregulated in the setting of persistent immune complexes in refractory disease.

Lyme disease affects people worldwide, with different *Bb* strains driving varying disease presentations globally. Given the potential for long-term morbidity associated with this infection in those that develop post-Lyme disease symptoms, there is an urgent need for biomarkers and mechanisms to help guide clinical care. Deep antibody profiling here points to the presence of compartment-specific *Bb* antibody profiles that both distinguish antibiotic-refractory LA and also point to the potential importance of reducing complement activation and attenuating inflammatory antibody activity as strategies to attenuate persistent inflammation and disease in the joints. Thus, additional studies are needed to investigate the generalizability of these observations across populations, as well as their potential role as mechanistic drivers of disease.

Limitations of the study

There are several important limitations to this study. First, the interval between start of antibiotics and sample acquisition differed between the refractory and responsive groups, where samples were collected at a later time in the refractory group (Table 1). Similarly, the cumulative exposure to antibiotics differed across the groups due to differences in typical clinical indication for joint fluid aspiration. In the responsive group, samples were collected prior to or during oral antibiotics. In the refractory group, sampling occurred before or soon after IV antibiotics, a time period when patients were still infected or soon thereafter, which limits the ability to determine antibody characteristics in the late post-infectious period. This difference in duration of inflammation or cumulative antibiotic exposure could lead to differences in antibody profiles. Thus, in the future, a study capturing samples earlier in infection or dynamically over time would be useful to define the impact of each of these factors as biomarkers and/or drivers of disease and could be used to explore the predictive capability of factors in determining ultimate antibiotic response. Secondly, as a negative control, it is not possible to include joint fluid from uninflamed, uninfected individuals since they do not have joint effusions. However, a useful comparison might be joint fluid from patients with osteoarthritis, a less inflammatory form of arthritis. Additionally, many of the lipoproteins studied here are polymorphic among different *Bb* strains/genotypes, and thus the source and strain of antigens and lysate used likely plays a role in their variable recognition by antibodies.[62]

STAR★METHODS

Detailed methods are provided in the online version of this paper and include the following:

- KEY RESOURCES TABLE
- RESOURCE AVAILABILITY
  - Lead contact
  - Materials availability
  - Data and code availability

SUPPLEMENTAL INFORMATION

Supplemental information can be found online at https://doi.org/10.1016/j.isci.2024.108804.

ACKNOWLEDGMENTS

We would like to acknowledge the support provided by the MGH ECOR Scholars Award (G.A.) and the Ragon Institute of MGH, MIT and Harvard for funding to support this project. We would also like to thank Dr. Mark Namchuk and the Malcolm and Emily Fairbairn Family Donor Advised Fund for supporting this work on Lyme disease, as well as Army ICB UARC Contract W911NF-19-D-0001 funding (D.A.L.). The graphical abstract was created with Biorender.com. Additionally, we would like to thank Dr. Ryan McNamara of the Ragone Institute Systems Serology lab for valuable conversations and insights.

AUTHOR CONTRIBUTIONS

Conceptualization and methodology: K.A.B., A.C.S., and G.A.; Investigation: K.A.B. and E.D.; Data curation: C.D.W., K.A.B., and A.C.S.; Formal analysis: C.D.W. and D.A.L.; Visualization: C.D.W., S.P., and K.A.B.; Writing – original draft: K.A.B.; Writing – review and editing: C.D.W., K.A.B., K.S., J.A.B., A.C.S., D.A.L., and G.A.; Resources: K.S., A.C.S., D.A.L., and G.A.; Supervision: J.A.B., A.C.S., D.A.L., and. G.A.

DECLARATION OF INTERESTS

G.A. is an equity holder in Systems Seromyx Inc. and Leyden Labs. G.A. is an employee of Moderna Inc. K.S. is an employee of Takeda Pharmaceuticals. J.A.B. has received research support from Analog Devices Inc., Pfizer Inc., and Zeus Scientific for other studies and has received personal fees for consulting work from DiaSorin, Roche Diagnostics, and T2 Biosystems.

Received: July 21, 2023
Revised: November 24, 2023
Accepted: January 2, 2024
Published: January 4, 2024

REFERENCES

1. Schwartz, A.M., Hinckley, A.F., Mead, P.S., Hook, S.A., and Kugeler, K.J. (2017). Surveillance for Lyme Disease - United States, 2008-2015. MMWR. Surveill. Summ. *66*, 1–12.
2. Hinckley, A.F., Connally, N.P., Meek, J.I., Johnson, B.J., Kemperman, M.M., Feldman, K.A., White, J.L., and Mead, P.S. (2014). Lyme disease testing by large commercial laboratories in the United States. Clin. Infect. Dis. *59*, 676–681.
3. Steere, A.C., and Sikand, V.K. (2003). The presenting manifestations of Lyme disease and the outcomes of treatment. N. Engl. J. Med. *348*, 2472–2474.
4. Arvikar, S.L., and Steere, A.C. (2015). Diagnosis and treatment of Lyme arthritis. Infect. Dis. Clin. *29*, 269–280.
5. Lantos, P.M., Rumbaugh, J., Bockenstedt, L.K., Falck-Ytter, Y.T., Aguero-Rosenfeld, M.E., Auwaerter, P.G., Baldwin, K., Bannuru, R.R., Belani, K.K., Bowie, W.R., et al. (2021). Clinical Practice Guidelines by the Infectious Diseases Society of America (IDSA), American Academy of Neurology (AAN), and American College of Rheumatology (ACR): 2020 Guidelines for the Prevention, Diagnosis and Treatment of Lyme Disease. Clin. Infect. Dis. *72*, 1–8.
6. Steere, A.C., and Angelis, S.M. (2006). Therapy for Lyme arthritis: strategies for the treatment of antibiotic-refractory arthritis. Arthritis Rheum. *54*, 3079–3086.
7. Lochhead, R.B., Arvikar, S.L., Aversa, J.M., Sadreyev, R.I., Strle, K., and Steere, A.C. (2019). Robust interferon signature and suppressed tissue repair gene expression in synovial tissue from patients with postinfectious, Borrelia burgdorferi-induced Lyme arthritis. Cell Microbiol. *21*, e12954.
8. Johnston, Y.E., Duray, P.H., Steere, A.C., Kashgarian, M., Buza, J., Malawista, S.E., and Askenase, P.W. (1985). Lyme arthritis. Spirochetes found in synovial microangiopathic lesions. Am. J. Pathol. *118*, 26–34.
9. Arvikar, S.L., and Steere, A.C. (2022). Lyme Arthritis. Infect. Dis. Clin. *36*, 563–577.
10. Li, X., McHugh, G.A., Damle, N., Sikand, V.K., Glickstein, L., and Steere, A.C. (2011). Burden and viability of Borrelia burgdorferi in skin and joints of patients with erythema migrans or lyme arthritis. Arthritis Rheum. *63*, 2238–2247.

11. Jutras, B.L., Lochhead, R.B., Kloos, Z.A., Biboy, J., Strle, K., Booth, C.J., Govers, S.K., Gray, J., Schumann, P., Vollmer, W., et al. (2019). Borrelia burgdorferi peptidoglycan is a persistent antigen in patients with Lyme arthritis. Proc. Natl. Acad. Sci. USA *116*, 13498–13507.
12. Lochhead, R.B., Strle, K., Arvikar, S.L., Weis, J.J., and Steere, A.C. (2021). Lyme arthritis: linking infection, inflammation and autoimmunity. Nat. Rev. Rheumatol. *17*, 449–461.
13. Londoño, D., Cadavid, D., Drouin, E.E., Strle, K., McHugh, G., Aversa, J.M., and Steere, A.C. (2014). Antibodies to endothelial cell growth factor and obliterative microvascular lesions in the synovium of patients with antibiotic-refractory lyme arthritis. Arthritis Rheumatol. *66*, 2124–2133.
14. Ordóñez, D., Lochhead, R.B., Strle, K., Pianta, A., Arvikar, S., Van Rhijn, I., Stemmer-Rachamimov, A., and Steere, A.C. (2023). Cell-Mediated Cytotoxicity in Lyme Arthritis. Arthritis Rheumatol. *75*, 782–793.
15. Danzer, H., Glaesner, J., Baerenwaldt, A., Reitinger, C., Lux, A., Heger, L., Dudziak, D., Harrer, T., Gessner, A., and Nimmerjahn, F. (2020). Human Fcgamma-receptor IIb modulates pathogen-specific versus self-reactive antibody responses in lyme arthritis. Elife *9*, e55319.
16. Barbour, A.G., Jasinskas, A., Kayala, M.A., Davies, D.H., Steere, A.C., Baldi, P., and Felgner, P.L. (2008). A genome-wide proteome array reveals a limited set of immunogens in natural infections of humans and white-footed mice with Borrelia burgdorferi. Infect. Immun. *76*, 3374–3389.
17. Kannian, P., McHugh, G., Johnson, B.J.B., Bacon, R.M., Glickstein, L.J., and Steere, A.C. (2007). Antibody responses to Borrelia burgdorferi in patients with antibiotic-refractory, antibiotic-responsive, or non-antibiotic-treated Lyme arthritis. Arthritis Rheum. *56*, 4216–4225.
18. Sulka, K.B., Strle, K., Crowley, J.T., Lochhead, R.B., Anthony, R., and Steere, A.C. (2018). Correlation of Lyme Disease-Associated IgG4 Autoantibodies With Synovial Pathology in Antibiotic-Refractory Lyme Arthritis. Arthritis Rheumatol. *70*, 1835–1846.
19. Lu, L.L., Chung, A.W., Rosebrock, T.R., Ghebremichael, M., Yu, W.H., Grace, P.S., Schoen, M.K., Tafesse, F., Martin, C., Leung, V., et al. (2016). A Functional Role for Antibodies in Tuberculosis. Cell *167*, 433–443.e14.
20. Kawahara, J.Y., Irvine, E.B., and Alter, G. (2019). A Case for Antibodies as Mechanistic Correlates of Immunity in Tuberculosis. Front. Immunol. *10*, 996.
21. Cockburn, I.A., and Seder, R.A. (2018). Malaria prevention: from immunological concepts to effective vaccines and protective antibodies. Nat. Immunol. *19*, 1199–1211.
22. Strle, K., Shin, J.J., Glickstein, L.J., and Steere, A.C. (2012). Association of a Toll-like receptor 1 polymorphism with heightened Th1 inflammatory responses and antibiotic-refractory Lyme arthritis. Arthritis Rheum. *64*, 1497–1507.
23. Vudattu, N.K., Strle, K., Steere, A.C., and Drouin, E.E. (2013). Dysregulation of CD4+CD25(high) T cells in the synovial fluid of patients with antibiotic-refractory Lyme arthritis. Arthritis Rheum. *65*, 1643–1653.
24. Strle, K., Sulka, K.B., Pianta, A., Crowley, J.T., Arvikar, S.L., Anselmo, A., Sadreyev, R., and Steere, A.C. (2017). T-Helper 17 Cell Cytokine Responses in Lyme Disease Correlate With Borrelia burgdorferi Antibodies During Early Infection and With Autoantibodies Late in the Illness in Patients With Antibiotic-Refractory Lyme Arthritis. Clin. Infect. Dis. *64*, 930–938.
25. Sanes, J.T., Costello, C.E., and Steere, A.C. (2023). Heightened Pro-inflammatory Glycosylation of Borrelia burgdorferi IgG Antibodies in Synovial Fluid in Patients with Antibiotic-Refractory Lyme Arthritis. Arthritis Rheumatol. *75*, 1263–1274.
26. Ohmi, Y., Ise, W., Harazono, A., Takakura, D., Fukuyama, H., Baba, Y., Narazaki, M., Shoda, H., Takahashi, N., Ohkawa, Y., et al. (2016). Sialylation converts arthritogenic IgG into inhibitors of collagen-induced arthritis. Nat. Commun. *7*, 11205.
27. Tibshirani, R. (1997). The lasso method for variable selection in the Cox model. Stat. Med. *16*, 385–395.
28. Cyster, J.G., and Allen, C.D.C. (2019). B Cell Responses: Cell Interaction Dynamics and Decisions. Cell *177*, 524–540.
29. Coburn, J., Garcia, B., Hu, L.T., Jewett, M.W., Kraiczy, P., Norris, S.J., and Skare, J. (2021). Lyme Disease Pathogenesis. Curr. Issues Mol. Biol. *42*, 473–518.
30. Skare, J.T., and Garcia, B.L. (2020). Complement Evasion by Lyme Disease Spirochetes. Trends Microbiol. *28*, 889–899.
31. Chen, J., Field, J.A., Glickstein, L., Molloy, P.J., Huber, B.T., and Steere, A.C. (1999). Association of antibiotic treatment-resistant Lyme arthritis with T cell responses to dominant epitopes of outer surface protein A of Borrelia burgdorferi. Arthritis Rheum. *42*, 1813–1822.
32. Kalish, R.A., Leong, J.M., and Steere, A.C. (1995). Early and late antibody responses to full-length and truncated constructs of outer surface protein A of Borrelia burgdorferi in Lyme disease. Infect. Immun. *63*, 2228–2235.
33. Malhotra, R., Wormald, M.R., Rudd, P.M., Fischer, P.B., Dwek, R.A., and Sim, R.B. (1995). Glycosylation changes of IgG associated with rheumatoid arthritis can activate complement via the mannose-binding protein. Nat. Med. *1*, 237–243.
34. Marcinkiewicz, A.L., Kraiczy, P., and Lin, Y.P. (2017). There Is a Method to the Madness: Strategies to Study Host Complement Evasion by Lyme Disease and Relapsing Fever Spirochetes. Front. Microbiol. *8*, 328.
35. Lin, Y.P., Diuk-Wasser, M.A., Stevenson, B., and Kraiczy, P. (2020). Complement Evasion Contributes to Lyme Borreliae-Host Associations. Trends Parasitol. *36*, 634–645.
36. Caine, J.A., and Coburn, J. (2016). Multifunctional and Redundant Roles of Borrelia burgdorferi Outer Surface Proteins in Tissue Adhesion, Colonization, and Complement Evasion. Front. Immunol. *7*, 442.
37. Kraiczy, P. (2016). Hide and Seek: How Lyme Disease Spirochetes Overcome Complement Attack. Front. Immunol. *7*, 385.
38. Holers, V.M., and Banda, N.K. (2018). Complement in the Initiation and Evolution of Rheumatoid Arthritis. Front. Immunol. *9*, 1057.
39. Solomon, S., Kassahn, D., and Illges, H. (2005). The role of the complement and the Fc gamma R system in the pathogenesis of arthritis. Arthritis Res. Ther. *7*, 129–135.
40. Theofilopoulos, A.N., Carson, D.A., Tavassoli, M., Slovin, S.F., Speers, W.C., Jensen, F.B., and Vaughan, J.H. (1980). Evidence for the presence of receptors for C3 and IgG Fc on human synovial cells. Arthritis Rheum. *23*, 1–9.
41. Lawrenz, M.B., Wooten, R.M., Zachary, J.F., Drouin, S.M., Weis, J.J., Wetsel, R.A., and Norris, S.J. (2003). Effect of complement component C3 deficiency on experimental Lyme borreliosis in mice. Infect. Immun. *71*, 4432–4440.
42. Ackerman, M.E., Crispin, M., Yu, X., Baruah, K., Boesch, A.W., Harvey, D.J., Dugast, A.S., Heizen, E.L., Ercan, A., Choi, I., et al. (2013). Natural variation in Fc glycosylation of HIV-specific antibodies impacts antiviral activity. J. Clin. Invest. *123*, 2183–2192.
43. Moore, J.S., Wu, X., Kulhavy, R., Tomana, M., Novak, J., Moldoveanu, Z., Brown, R., Goepfert, P.A., and Mestecky, J. (2005). Increased levels of galactose-deficient IgG in sera of HIV-1-infected individuals. AIDS *19*, 381–389.
44. Chakraborty, S., Gonzalez, J., Edwards, K., Mallajosyula, V., Buzzanco, A.S., Sherwood, R., Buffone, C., Kathale, N., Providenza, S., Xie, M.M., et al. (2021). Proinflammatory IgG Fc structures in patients with severe COVID-19. Nat. Immunol. *22*, 67–73.
45. Petrović, T., Alves, I., Bugada, D., Pascual, J., Vučković, F., Skelin, A., Gaifem, J., Villar-Garcia, J., Vicente, M.M., Fernandes, Â., et al. (2021). Composition of the immunoglobulin G glycome associates with the severity of COVID-19. Glycobiology *31*, 372–377.
46. Hoepel, W., Chen, H.J., Geyer, C.E., Allahverdiyeva, S., Manz, X.D., de Taeye, S.W., Aman, J., Mes, L., Steenhuis, M., Griffith, G.R., et al. (2021). High titers and low fucosylation of early human anti-SARS-CoV-2 IgG promote inflammation by alveolar macrophages. Sci. Transl. Med. *13*, eabf8654.
47. Larsen, M.D., de Graaf, E.L., Sonneveld, M.E., Plomp, H.R., Nouta, J., Hoepel, W., Chen, H.J., Linty, F., Visser, R., Brinkhaus, M., et al. (2021). Afucosylated IgG characterizes enveloped viral responses and correlates with COVID-19 severity. Science *371*, eabc8378.
48. Reily, C., Stewart, T.J., Renfrow, M.B., and Novak, J. (2019). Glycosylation in health and disease. Nat. Rev. Nephrol. *15*, 346–366.
49. Tomana, M., Schrohenloher, R.E., Reveille, J.D., Arnett, F.C., and Koopman, W.J. (1992). Abnormal galactosylation of serum IgG in patients with systemic lupus erythematosus and members of families with high frequency of autoimmune diseases. Rheumatol. Int. *12*, 191–194.
50. Vučković, F., Krištić, J., Gudelj, I., Teruel, M., Keser, T., Pezer, M., Pučić-Baković, M., Štambuk, J., Trbojević-Akmačić, I., Barrios, C., et al. (2015). Association of systemic lupus erythematosus with decreased immunosuppressive potential of the IgG glycome. Arthritis Rheumatol. *67*, 2978–2989.
51. Rombouts, Y., Ewing, E., van de Stadt, L.A., Selman, M.H.J., Trouw, L.A., Deelder, A.M., Huizinga, T.W.J., Wuhrer, M., van Schaardenburg, D., Toes, R.E.M., and Scherer, H.U. (2015). Anti-citrullinated protein antibodies acquire a pro-inflammatory Fc glycosylation phenotype prior to the onset of rheumatoid arthritis. Ann. Rheum. Dis. *74*, 234–241.
52. Ercan, A., Cui, J., Chatterton, D.E.W., Deane, K.D., Hazen, M.M., Brintnell, W., O'Donnell, C.I., Derber, L.A., Weinblatt, M.E., Shadick, N.A., et al. (2010). Aberrant IgG galactosylation precedes disease onset, correlates with disease activity, and is prevalent in autoantibodies in rheumatoid arthritis. Arthritis Rheum. *62*, 2239–2248.
53. van Zeben, D., Rook, G.A., Hazes, J.M., Zwinderman, A.H., Zhang, Y., Ghelani, S.,

Rademacher, T.W., and Breedveld, F.C. (1994). Early agalactosylation of IgG is associated with a more progressive disease course in patients with rheumatoid arthritis: results of a follow-up study. Br. J. Rheumatol. *33*, 36–43.
54. Bartsch, Y.C., Rahmöller, J., Mertes, M.M.M., Eiglmeier, S., Lorenz, F.K.M., Stoehr, A.D., Braumann, D., Lorenz, A.K., Winkler, A., Lilienthal, G.M., et al. (2018). Sialylated Autoantigen-Reactive IgG Antibodies Attenuate Disease Development in Autoimmune Mouse Models of Lupus Nephritis and Rheumatoid Arthritis. Front. Immunol. *9*, 1183.
55. Brückner, C., Lehmann, C., Dudziak, D., and Nimmerjahn, F. (2017). Sweet SIGNs: IgG glycosylation leads the way in IVIG-mediated resolution of inflammation. Int. Immunol. *29*, 499–509.
56. Pagan, J.D., Kitaoka, M., and Anthony, R.M. (2018). Engineered Sialylation of Pathogenic Antibodies In Vivo Attenuates Autoimmune Disease. Cell *172*, 564–577.e13.
57. Kalish, R.A., Leong, J.M., and Steere, A.C. (1993). Association of treatment-resistant chronic Lyme arthritis with HLA-DR4 and antibody reactivity to OspA and OspB of Borrelia burgdorferi. Infect. Immun. *61*, 2774–2779.
58. Shin, J.J., Strle, K., Glickstein, L.J., Luster, A.D., and Steere, A.C. (2010). Borrelia burgdorferi stimulation of chemokine secretion by cells of monocyte lineage in patients with Lyme arthritis. Arthritis Res. Ther. *12*, R168.
59. Breedveld, A., and van Egmond, M. (2019). IgA and FcalphaRI: Pathological Roles and Therapeutic Opportunities. Front. Immunol. *10*, 553.
60. Aleyd, E., van Hout, M.W.M., Ganzevles, S.H., Hoeben, K.A., Everts, V., Bakema, J.E., and van Egmond, M. (2014). IgA enhances NETosis and release of neutrophil extracellular traps by polymorphonuclear cells via Fcalpha receptor I. J. Immunol. *192*, 2374–2383.
61. Bos, A., Aleyd, E., van der Steen, L.P.E., Winter, P.J., Heemskerk, N., Pouw, S.M., Boon, L., Musters, R.J.P., Bakema, J.E., Sitaru, C., et al. (2022). Anti-FcalphaRI Monoclonal Antibodies Resolve IgA Autoantibody-Mediated Disease. Front. Immunol. *13*, 732977.
62. Aguero-Rosenfeld, M.E., Wang, G., Schwartz, I., and Wormser, G.P. (2005). Diagnosis of lyme borreliosis. Clin. Microbiol. Rev. *18*, 484–509.
63. Wharton, M., Chorba, T.L., Vogt, R.L., Morse, D.L., and Buehler, J.W. (1990). Case definitions for public health surveillance. MMWR Recomm. Rep. (Morb. Mortal. Wkly. Rep.) *39*, 1–43.
64. Steere, A.C., Grodzicki, R.L., Kornblatt, A.N., Craft, J.E., Barbour, A.G., Burgdorfer, W., Schmid, G.P., Johnson, E., and Malawista, S.E. (1983). The spirochetal etiology of Lyme disease. N. Engl. J. Med. *308*, 733–740.
65. Fung, B.P., McHugh, G.L., Leong, J.M., and Steere, A.C. (1994). Humoral immune response to outer surface protein C of Borrelia burgdorferi in Lyme disease: role of the immunoglobulin M response in the serodiagnosis of early infection. Infect. Immun. *62*, 3213–3221.
66. Brown, E.P., Dowell, K.G., Boesch, A.W., Normandin, E., Mahan, A.E., Chu, T., Barouch, D.H., Bailey-Kellogg, C., Alter, G., and Ackerman, M.E. (2017). Multiplexed Fc array for evaluation of antigen-specific antibody effector profiles. J. Immunol. Methods *443*, 33–44.
67. Brown, E.P., Licht, A.F., Dugast, A.S., Choi, I., Bailey-Kellogg, C., Alter, G., and Ackerman, M.E. (2012). High-throughput, multiplexed IgG subclassing of antigen-specific antibodies from clinical samples. J. Immunol. Methods *386*, 117–123.
68. Ackerman, M.E., Moldt, B., Wyatt, R.T., Dugast, A.S., McAndrew, E., Tsoukas, S., Jost, S., Berger, C.T., Sciaranghella, G., Liu, Q., et al. (2011). A robust, high-throughput assay to determine the phagocytic activity of clinical antibody samples. J. Immunol. Methods *366*, 8–19.
69. Karsten, C.B., Mehta, N., Shin, S.A., Diefenbach, T.J., Slein, M.D., Karpinski, W., Irvine, E.B., Broge, T., Suscovich, T.J., and Alter, G. (2019). A versatile high-throughput assay to characterize antibody-mediated neutrophil phagocytosis. J. Immunol. Methods *471*, 46–56.
70. Fischinger, S., Fallon, J.K., Michell, A.R., Broge, T., Suscovich, T.J., Streeck, H., and Alter, G. (2019). A high-throughput, bead-based, antigen-specific assay to assess the ability of antibodies to induce complement activation. J. Immunol. Methods *473*, 112630.
71. Westerhuis, J.A., van Velzen, E.J.J., Hoefsloot, H.C.J., and Smilde, A.K. (2010). Multivariate paired data analysis: multilevel PLSDA versus OPLSDA. Metabolomics *6*, 119–128.

STAR★METHODS

KEY RESOURCES TABLE

REAGENT or RESOURCE	SOURCE	IDENTIFIER
Antibodies		
Mouse anti-human IgG1 Fc-PE	Southern Biotech	Cat# 9054-09; RRID: AB_2796628
Mouse anti-human IgG2 Fc-PE	Southern Biotech	Cat# 9060-09; RRID: AB_2796635
Mouse Anti-Human IgG3-Hinge PE	Southern Biotech	Cat# 9210-09; RRID: AB_2796701
Mouse anti-human IgG4 Fc-PE	Southern Biotech	Cat# 9200-09; RRID: AB_2796693
Mouse anti-human IgA1 Fc-PE	Southern Biotech	Cat# 9130-09; RRID: AB_2796656
Mouse anti-human IgM Fc-PE	Southern Biotech	Cat# 9020-09; RRID: AB_2796577
Anti-guinea pig complement C3 goat IgG fraction, fluorescein-conjugated	MP Biomedicals	Cat# MP0855385; RRID: AB_2334913
Anti-CD66b PacBlue	Biolegend	Cat# 305112; clone: G10F5; RRID: AB_2563294
Biological samples		
Cohort of human serum and joint fluid samples	Allen Steere; Massachusetts General Hospital	N/A
Chemicals, peptides, and recombinant proteins		
B67 culture lysate	Provided by Allen Steere, MD; Massachusetts General Hospital[64,65]	N/A
CRASP1	Rockland	Cat# 000-001-C18
CRASP2	Rockland	Cat# 000-001-C19
DbpA	Rockland	Cat# 000-001-B98
DbpB	Rockland	Cat# 000-001-C16
Arp37	Rockland	Cat# 000-001-C09
flagellin	Rockland	Cat# 000-001-C14
OspA	Rockland	Cat# 000-001-C13
OspB	Rockland	Cat# 000-001-C15
OspC	Rockland	Cat# 000-001-C11
OspE	Rockland	Cat# 000-001-C10
p27	Rockland	Cat# 000-001-C30
p35	Rockland	Cat# 000-001-C12
p39	Rockland	Cat# 000-001-C17
VlsE	Rockland	Cat# 000-001-C33
ApoB100	R&D Systems	Cat# AF3260-SP
HA Influenza B (B/Massachusetts/03/2010) Hemagglutinin / HA protein (His Tag)	Immunetech	Cat# 40191-V08B
HA(dTM) (H1N1/A/New Caledonia/20/99) Hemagglutinin / HA protein (His Tag)	Immunetech	Cat# IT-003-001ΔTMp
HA(A/Hong Kong/4801/2014)(H3N2)	Immunetech	Cat# IT-003-00430ΔTMp
recombinant EBOV Soluble GP	ibt bioservices	Cat# 0565-001
sulfo-NHS (N-hydroxysulfosuccinimide)	Thermo Fisher Scientific	Cat# A39269
ethyl dimethylaminopropyl carbodiimide hydrochloride (EDC)	Thermo Fisher Scientific	Cat# A35391
Sambucus Nigra Lectin (SNA, EBL), Fluorescein	Vectorlabs	Cat# FL-1301-2

(*Continued on next page*)

Continued

REAGENT or RESOURCE	SOURCE	IDENTIFIER
Ricinus Communis Agglutinin I (RCA I, RCA120), Fluorescein	Vectorlabs	Cat# FL-1081-5
Avi-Tagged Human Fc Receptors (Fcγ2A, Fcγ2B, Fcγ3A and Fcγ3B)	Produced by Duke Protein Production facility	N/A
Tetanus toxoid	MassBiologics	Lot# Lp1099p
sulfo-NHS-LC-LC biotin	Thermo Fisher Scientific	Cat# A35358
veronal buffer supplemented with 0.1% fish skin gelatin	Boston Bio Products	Cat# IBB-290X
Streptavidin-R-Phycoerythrin	Prozyme	Cat# PJ31S
Critical commercial assays		
BirA biotin-protein ligase reaction kit	Avidity	Cat# BirA500
Deposited data		
Generated code	This paper	Zenodo: https://doi.org/10.5281/zenodo.10257968
Experimental models: Cell lines		
THP-1 human monocyte cell line	ATCC	Cat# TIB-202; RRID: CVCL_0006
Software and algorithms		
R programming language	Version 4.0.3	https://www.r-project.org/
ForeCyt software	Sartorius	https://www.sartorius.com/en/products/flow-cytometry/flow-cytometry-software
Other		
Fluospheres™ NeutrAvidin™-Labeled Microspheres, 1.0 µm, red fluorescent (580/605), 1% solids	Invitrogen	Cat# F8775
FluoSpheres™ NeutrAvidin™-Labeled Microspheres, 1.0 µm, yellow-green fluorescent (505/515), 1% solids	Invitrogen	Cat# F8776
Zeba Spin Desalting Column, 7 MWCO	ThermoFisher Scientific	Cat#: 89877
Magplex microspheres	Luminex Corporation	Cat#s: MC12001-01, MC12003-01, MC12004-01, MC12005-01, MC12012-01, MC12015-01, MC12020-01, MC12023-01, MC12024-01, MC12026-01, MC12027-01, MC12039-01, MC12040-01, MC12044-01, MC12046-01, MC12055-01, MC12062-01
Low-tox guinea pig complement	CedarLane	Cat# CL4051

RESOURCE AVAILABILITY

Lead contact

Further information and requests for resources and reagents should be directed to and will be fulfilled by the lead contact, Galit Alter (galit.alter@modernatx.com).

Materials availability

This study did not generate new unique reagents.

Data and code availability

- All data generated during this study is available upon reasonable request.
- All code generated during this study has been deposited in Zenodo and is publicly available as of the date of publication. The DOI is listed in the key resources table.
- Any additional information required to reanalyze the data reported in this paper is available from the lead contact upon request.

EXPERIMENTAL MODEL AND STUDY PARTICIPANT DETAILS

Study cohort

Serum and joint fluid samples were included from 31 patients with antibiotic-refractory and 11 with antibiotic-responsive LA (Table 1). These patients were seen at Massachusetts General Hospital by Dr. Allen Steere between 2005 and 2018 except for 3 patients who were seen in between 1992 and 1998 at Tufts Medical Center. The Human Investigations Committee at Massachusetts General Hospital (MGH) and Tufts Medical Center approved the study, titled "Immunity in Lyme Disease", and all patients (including parents of patients ages 12-18) provided written informed consent. All LA patients met Centers for Disease Control and Prevention criteria for Lyme disease.[63] "Antibiotic-refractory" patients were defined as those for whom oral antibiotics alone or followed by intravenous antibiotics did not resolve their synovitis. Serum and joint fluid were obtained at the same visit for each patient.

In the 11 patients with antibiotic-responsive LA, serum and joint fluid samples were collected before or during oral antibiotic therapy. In 10 of 31 patients with antibiotic-refractory LA, these samples were obtained a median duration of 2 weeks prior to IV antibiotic therapy, when knees were typically very swollen. In the remaining 21 refractory patients, the samples were collected a median duration of 4 weeks after the conclusion of IV therapy when joint fluid was still obtainable. Because the results of antibody testing were similar in the subgroups with antibiotic-refractory LA and to bolster group size for statistical analysis, these 2 subgroups were combined for presentation here.

In the antibiotic-responsive LA group, 2/11 patients identified as female, vs 14/31 for the antibiotic-refractory LA group. While the ratio of female to male patients differed between groups, multivariate analysis did not identify humoral differences between sexes within the respective groups (data not shown). However, it is possible that sex differences are present but not observable at these sample sizes. Information on ancestry, race and ethnicity, and socioeconomic status was not gathered at the time of sample acquisition and so is not discussed here.

Cell lines

THP-1 cells (ATCC, RRID:CVCL_0006, male) a human acute monocytic leukemia cell line, were grown at 37C, 5% CO2 in RPMI with 10% fetal bovine serum, L-glutamine, penicillin/streptomycin, HEPES and beta-mercaptoethanol, and used for assays at low passage number. The THP-1 cell line was authenticated by ATCC with STR profiling, and no mycoplasma contamination was detected.

Primary immune cells

Human neutrophils were isolated from fresh peripheral blood. Peripheral blood was collected by the MGH Blood Bank or by the Ragon Institute from healthy volunteers under protocol. All volunteers were over 18 years of age and gave signed consent. Samples were de-identified before use. The study was approved by the MGH Institutional Review Board. Human neutrophils were maintained in R10 (RPMI with 10% fetal bovine serum, L-glutamine, penicillin/streptomycin and HEPES) and grown at 37C, 5% CO2 for the duration of the assay.

METHOD DETAILS

Antigens

Antigens used for Luminex based assays included B67 culture lysate (derived from G39/40, kindly provided by Allen Steere, Massachusetts General Hospital), *Bb* CRASP1, CRASP2, DbpA, DbpB, Arp37, flagellin, OspA, OspB, OspC, OspE, p27, p35, p39, VlsE (all from Rockland), ApoB100 (R&D Systems), HA (Immunetech), and EBOV (ibt bioservices). All of the commercially available *B.burgorferi* antigens utilized were derived from strain B31 (Strain ATCC 35210/DSM4680/CIP 102532/B31). The B67 culture lysate is a sonicate derived from strain G39/40, a tick isolate recovered in 1983 in Guilford, Connecticut.[64,65]

Luminex profiling

A multiplexed Luminex assay was used to determine relative titer of antigen-specific isotypes, subclasses, Lectin-binding, FcγR binding.[66,67] Antigens were covalently linked to carboxyl-modified Magplex Luminex beads (Luminex Corp) using Sulfo-NHS (N-hydroxysulfosuccinimide, Thermo Fisher Scientific) and ethyl dimethylaminopropyl carbodiimide hydrochloride (EDC, Thermo Fisher Scientific). Antigen-coupled microspheres were blocked, washed, resuspended in PBS, and stored at 4°C. To form immune complexes, antigen-coupled beads were incubated with appropriately diluted plasma and joint fluid (1:10 for IgG1/2/3/41:100 for all low-affinity FcγRs) overnight at 4°C, shaking at 700 rpm. The following day, plates were washed with 0.1% BSA 0.02% Tween-20. PE-coupled mouse anti-human detection antibodies (Southern Biotech) were used to detect antigen-specific antibody binding. For detection of sialic acid and galactose, fluorescein-labeled plant-based lectin detects, SNA and RCA (Vectorlabs), were added as detection reagents at a 1:100 (SNA) and 1:500 dilution (RCA). For the detection of FcR binding, Avi-Tagged FcRs (Fcγ2A, Fcγ2B, Fcγ3A and Fcγ3B; Duke Protein Production facility) were biotinylated using BirA500 kit

(Avidity) per manufacturer's instructions. Biotinylated FcRs were tagged with PE and added to immune complexes. Fluorescence was acquired using an Intellicyt iQue, and relative antigen-specific antibody titer and FcR binding is reported as Median Fluorescence Intensity (MFI).

Functional assays

Antibody-dependent cellular phagocytosis (ADCP), antibody-dependent neutrophil phagocytosis (ADNP), and antibody-dependent complement deposition (ADCD) were performed.[68–70] Antigens used for ADCP and ADNP assays were: DbpA, DbpB, p35, p39, p66, VlsE, flagellin, and B67 culture lysate. Antigens used for ADCD assays included B67 culture lysate (kindly provided by Allen Steere, Massachusetts General Hospital), CRASP1, CRASP2, DbpA, DbpB, Arp37, flagellin, OspA, OspB, OspC, OspE, p27, p35, p39, VlsE (all from Rockland), ApoB100 (R&D Systems), HA (Immunetech), tetanus toxoid (MassBiologics), and EBOV (ibt bioservices). Antigen was biotinylated using Sulfo-NHS-LC-LC biotin (Thermo) and desalted using Zeba Columns (Thermo). Yellow-green (for ADCP and ADNP) or red (for ADCD) were incubated with biotinylated antigen for 2 hours at 37C or overnight at 4°C. Coupled beads were washed twice with 0.01% BSA in PBS and resuspended at a concentration of 10ug/mL. To form immune complexes, antigen-coupled beads were added to 96-well plates with an equal volume of appropriately diluted plasma and joint fluid (1:10 for ADCD, 1:20 for ADCP and ADNP) and incubated for 2 hours at 37C. Immune complexes were washed following incubation. For ADCP, 1.25x105 THP-1 cells/mL were added to immune complexes and incubated for 16-18 hours at 37C. Following the incubation, cells were fixed with 4% PFA. For ADNP, white blood cells were isolated from whole blood from healthy donors using ammonium-chloride potassium lysis to lyse red blood cells. 2.5x105 cells/mL were added to immune complexes and incubated for 1 hour at 37C. Neutrophils were stained with an anti-CD66b PacBlue (Biolegend) detection antibody and fixed with 4% PFA. For ADCD, lyophilized guinea pig complement (Cedarlane) was resuspended according of manufacturer's recommendations and diluted in gelatin veronal buffer supplemented with calcium and magnesium (Boston BioProducts). The diluted complement was added to immune complexes and incubated at 37C for 20 minutes. C3 deposition was detected using an anti-C3 fluorescein-conjugated goat IgG fraction detection antibody (Mpbio).

Fluorescence for the functional assays was acquired using an iQue (Intellicyt). For phagocytosis assays, a phagocytic score was calculated using the following formula: (percentage of bead-positive cells) x (GeoMean of MFI of bead-positive cells)/10,000. ADCD is reported as median MFI of C3 deposition.

QUANTIFICATION AND STATISTICAL ANALYSIS

Univariate analyses

All univariate plots were visualized and analyzed using R (version 4.0.3). Univariate plots show the $\log_{10}$ MFI values for functional assays and Luminex assays, visualized as boxplots with median denoted. Unless otherwise noted, statistical significance between measurements was assessed using the Mann-Whitney nonparametric test, with p-values then corrected for multiple hypothesis testing via Benjamini-Hochburg. When comparing proportions, a Fisher's exact test was utilized, with p-values corrected for multiple hypothesis testing via Benjamini-Hochburg. Heatmaps were generated via the 'pheatmap' command in the package 'pheatmap' (v 1.0.12). Figures were edited only for page positioning, legend color, and size in Adobe Illustrator (v2020) for clearer visualization.

Multivariate data Pre-processing

With the exception of univariate analyses, all analysis started with background correction by PBS. 2x the mean raw score of 2 PBS controls was subtracted from all measurements to control for background noise. Any negative calculated value was functionally considered to be zero. All features were mean-centered and scaled to unit variance. MFI values for Luminex and lectin assays and the ADCD functional assay were transformed into $\log_{10}$ values. Features with >50% zero values were removed from the dataset for multivariate analyses.

Pan-antigen analyses

Pan-antigen scores were calculated through mean-centering and scaling all data to unit variance by antigen and then summing scaled antigen values by sample. Univariate pan-antigen plots show the pan-antigen scores for functional assays and Luminex assays, visualized as boxplots with median denoted. Statistical significance was assessed with a nonparametric Wilcoxon signed-rank test to account for paired samples and corrected for multiple hypothesis testing via Benjamini-Hochburg.

Multivariate analyses

Multivariate analyses included lectin, Luminex, and functional antibody measurements. For unpaired classification models, partial least squares discriminant analysis (PLSDA) was performed on the data after feature reduction via LASSO regularization and variable selection. LASSO variable selection was performed via the LASSO feature selection algorithm, which was run 100 times on the entire dataset using the function 'select_lasso' from the 'systemsseRology' R package (v1.1). Features selected in 80% or more of the 100 rounds were used in the final model. Feature selection was implemented to reduce the risk of overfitting the models due to the large number of available features.

Multilevel partial least squares discriminant analysis (mPLSDA) was performed for all classification models separating joint fluid and serum samples from the same individual. mPLSDA generates models that better account for the paired nature of samples than does standard PLSDA.[71] mPLSDA models were built using data after feature reduction via LASSO regularization and variable selection was performed. Both PLSDA and mPLSDA models were implemented using the R 'systemsseRology' package (v1.1).

PLSDA and mPLSDA classification model performances were assessed using a five-fold cross validation approach and reported cross-validation accuracy is the mean of 10 rounds of 5-fold cross validation. Each round includes 100 repeats of feature selection per fold. To assess the importance of selected features, negative control models were built both by permuting group labels and by selecting random, size-matched features in place of true selected features. 10 rounds of cross-validation with 5 permutation and 5 random-feature trials per round (again with 100 repeats of feature selection per fold per round for the permutation trials) were performed, and exact P values were obtained from the tail probability of the generated null distribution. For PLSDAs, negative control models were also built by assigning all samples to the larger class, and repeating 10 rounds of 5-fold cross-validation with 100 repeats of feature selection per fold per round. For the responsive mPLSDA model, an additional null model was built by selecting random features from a pool of features with features highly (Spearman's $R > |0.8|$) correlated with selected features removed. All multivariate analyses were visualized and analyzed using R (version 4.0.3).

Correlation networks

Correlation networks were built to reveal additional serology features significantly associated with the selected features. Serology features significantly ($P < 0.05$, after a Benjamini-Hochberg correction) correlated (Spearman $r > |0.7|$) via Spearman correlation were selected as co-correlates. Correlation coefficients were calculated using the 'correlate' function in the 'Corrr' package (v0.4.3), with p values corrected using 'p.adjust' from the 'stats' package (v4.0.3). Network visualization was performed using 'ggraph' (v2.0.5) and 'igraph' (v1.2.6) packages, with manual label and node positioning corrections made in Adobe Illustrator (v2020) for improved visualization. The gradient color of edges represents correlation value between the features, represented as nodes. Nodes are colored according to selected status, with colored nodes as selected features colored by group in which those features are enriched and white nodes as co-correlate features.

ROC and AUC

Receiver-operator curves (ROC) were generated using the function 'roc' in the 'pROC' package (v 1.18.0). 100 trials of 5-fold CV for each model were run and the resultant ROCs visualized. The numerical mean area-under-the-curve (AUC) is also reported on each figure.